Analysis on the exclusiveness of turbulence suppression between static and time-varying shear flow

Y. Z. Zhang,[1,a)] T. Xie,[2] and S. M. Mahajan[3]
[1]*Center for Magnetic Fusion Theory, Chinese Academy of Sciences, Hefei China*
[2]*Southwestern Institute of Physics, Chengdu, China*
[3]*Institute for Fusion Studies, University of Texas at Austin, Austin, Texas 78712, USA*

(Received 13 September 2011; accepted 4 November 2011; published online 3 February 2012)

The analytical theory of turbulence suppression by shear flow [Y. Z. Zhang and S. M. Mahajan, Phys. Fluids B **4**, 1385 (1992)] is extended to analyze the combined actions of flows that have time-varying as well as static components. It is found that each component, appearing alone, may yield the same suppression level. However, when both components co-exist, either tends to diminish the suppression caused by the other in certain parameter ranges—a conclusion that agrees with recently published simulation results by Maeyama *et al*. [Phys. Plasmas **17**, 062305 (2010)]. In particular, the mutual exclusiveness is maximized as the strengths of the two components become comparable. The adopted averaging method of the asymptotic theory reveals that it is the coupling between the time-varying shear flow and the induced time-varying relative orbit motion that causes the asymmetry of the two components in turbulence suppression. The numerical results based on a Floquet analysis are also presented for comparison. The implications of the theory to L-H transition on tokamaks are discussed, especially, regarding experimental observations of the disappearance of the geodesic acoustic mode in H phases. © *2012 American Institute of Physics*.
[doi:10.1063/1.3676597]

Zonal flows have been investigated in great detail by the magnetic fusion community because of their possible role in the suppression of drift wave turbulence believed to induce anomalous transport in tokamaks.[1] Two different types of zonal flows, each possessing the shear flow structure required for turbulence suppression, are observed: (1) the zero mean frequency zonal flow (ZMF), typically in the frequency range of 0–10 kHz and (2) the geodesic acoustic mode (GAM) typically in the frequency range >10 kHz. The theories of turbulence suppression in early days were worked out for static shear flows only.[2–4] After the discovery of the zonal flow, the theories were extended to time-varying flows limited, however, to a single frequency and without a co-existing static component.[5]

Finding an answer to the interesting question of how turbulent transport will be affected if the two types of shear flows were to appear simultaneously is the main thrust of this paper. In the static category, we include not only purely static shear flows but also approximate ZMFs if their time scales are well separated from the GAMs. One could imagine, for instance, that the combined effect would always be enhanced suppression. The answer, however, turns out to be not so simple. In the published literature (numerical simulation[6] and analytical theory[7]), it is found that as regards the turbulence suppression, the two different types of shear flows are often in conflict over a wide parameter range. In particular, the combined suppression is minimized if the strengths of the two shear flows are comparable. The present brief article draws heavily from Ref. 7; detailed numerical solutions, based on a Floquet analysis of two-point orbit correlation theory, are presented, and the relevance of the theoretical results to experimental observations in L-H transition is discussed.

The two-point orbit correlation theory used for static shear flow in Refs. 2–4 can also be applied to time varying shear flow as long as the time variation is much slower than the drift wave frequency. All the definitions in the basic equation set (Eq. (2) of Ref. 4),

$$\left(\frac{\partial}{\partial\tau}-1\right)\langle X_-^2(\tau)\rangle = 3\left\langle \overline{Y}_-^2(\tau)\right\rangle,$$
$$\left(\frac{\partial}{\partial\tau}-1\right)\left\langle \overline{Y}_-^2(\tau)\right\rangle = 3\langle X_-^2(\tau)\rangle + 16\sigma\langle X_-(\tau)\overline{Y}_-(\tau)\rangle,$$
$$\left(\frac{\partial}{\partial\tau}+2\right)\langle X_-(\tau)\overline{Y}_-(\tau)\rangle = 8\sigma\langle X_-^2(\tau)\rangle, \quad (1)$$

are the same as in the corresponding ones in Ref. 4 with the only exception that

$$\sigma \equiv \overline{\sigma}+\widetilde{\sigma} \rightarrow \overline{\sigma}+|\widetilde{\sigma}|\cos\omega t, \quad \omega << \omega_{\mathrm{DriftWave}} \quad (2)$$

has an oscillatory part.

In the preceding equations, $\langle X_-^2(\tau)\rangle$, $\left\langle \overline{Y}_-^2(\tau)\right\rangle$, $\langle X_-(\tau)\overline{Y}_-(\tau)\rangle$ are the orbit correlations for the relative distance of the two fluid elements in the radial and poloidal direction; $\overline{Y}_-(\tau)\equiv Y_-(\tau)/\alpha$, α describes the shear (dv_E/dr) induced anisotropic deformation of the turbulence spectrum in y-direction; $\sigma \equiv (dv_E/dr)/4\alpha D\langle k_\perp^2\rangle$; $\tau \equiv tD\langle k_\perp^2\rangle/2$, where t is the laboratory time, D is the turbulence diffusion

a)Author to whom correspondence should be addressed. Electronic mail: zhang_yz@ipp.ac.cn.

coefficient, dv_E/dr is the shearing rate, and $\langle k_\perp^2 \rangle$ is the ensemble averaged of the square of the perpendicular wave number.

Splitting the orbit correlation into its static and oscillatory parts,

$$\langle X_-^2(\tau)\rangle \to \langle X_-^2(\tau)\rangle_s + \langle X_-^2(\tau)\rangle_o, \tag{3}$$

and time averaging over Eq. (1) yields

$$\sigma\langle X_-(\tau)\overline{Y}_-(\tau)\rangle \to \overline{\sigma}\langle X_-(\tau)\overline{Y}_-(\tau)\rangle_s + \overline{\widetilde{\sigma}\langle X_-(\tau)\overline{Y}_-(\tau)\rangle_o},$$
$$\sigma\langle X_-^2(\tau)\rangle \to \overline{\sigma}\langle X_-^2(\tau)\rangle_s + \overline{\widetilde{\sigma}\langle X_-^2(\tau)\rangle_o}, \tag{4}$$
$$\overline{\sigma}\langle X_-^2(\tau)\rangle_o + \widetilde{\sigma}\langle X_-^2(\tau)\rangle_s + \widetilde{\sigma}\langle X_-^2(\tau)\rangle_o - \overline{\widetilde{\sigma}\langle X_-^2(\tau)\rangle_o}$$
$$\approx \overline{\sigma}\langle X_-^2(\tau)\rangle_o + \widetilde{\sigma}\langle X_-^2(\tau)\rangle_s. \tag{5}$$

In order to derive these equations, we have adopted the well-known Bogoliubov-Mitropolsky asymptotic averaging method[8] (with higher harmonics neglected).

In this way, we retain only the linear response of the oscillatory orbit correlation to $\widetilde{\sigma}$, which, in turn, can be solved to calculate the quadratic coupling to $\widetilde{\sigma}$. It is this coupling that makes the contribution from the oscillatory component not in unison with that from the static one. After straightforward algebra (solve the oscillatory orbit correlation as expressed in terms of $\widetilde{\sigma}$ and substitute them back to the averaged equations), one obtains the following set of equations (the subscript s of orbit correlation has been omitted):

$$\left(\frac{\partial}{\partial\tau} - 1\right)\langle X_-^2(\tau)\rangle = 3\left\langle \overline{Y}_-^2(\tau)\right\rangle,$$
$$\left(\frac{\partial}{\partial\tau} - 1\right)\left\langle \overline{Y}_-^2(\tau)\right\rangle = (3+\Delta_1)\langle X_-^2(\tau)\rangle + 16\sigma^*\langle X_-(\tau)\overline{Y}_-(\tau)\rangle,$$
$$\left(\frac{\partial}{\partial\tau} + 2 + \Delta_2\right)\langle X_-(\tau)\overline{Y}_-(\tau)\rangle = 8\sigma^*\langle X_-^2(\tau)\rangle, \tag{6}$$

where

$$\sigma^* \equiv \overline{\sigma}(1-\Delta_3), \quad \kappa \equiv 12+\omega^2, \quad \eta \equiv 16 + \frac{3}{2}(16\overline{\sigma})^2,$$
$$\Delta_1 \equiv \frac{16^2}{4}\frac{\eta(8+\omega^2)+2\kappa\omega^2}{\eta^2+\kappa^2\omega^2}|\widetilde{\sigma}|^2,$$
$$\Delta_2 \equiv \frac{3}{4}16^2\frac{2\eta+\kappa\omega^2}{\eta^2+\kappa^2\omega^2}|\widetilde{\sigma}|^2,$$
$$\Delta_3 \equiv \frac{3}{4}\frac{16^2\eta}{\eta^2+\kappa^2\omega^2}|\widetilde{\sigma}|^2.$$

The characteristic equation of Eq. (6) can be cast into the following form:

$$\left[(P-1)\left(P+\frac{1}{2}\right) - \frac{3\Delta_1}{16}\right]\left(P+\frac{1}{2}+\frac{\Delta_2}{4}\right) = 6(1-\Delta_3)^2\overline{\sigma}^2, \tag{7}$$

where $P^{-1} \equiv \langle\psi^2\rangle/\langle\psi^2\rangle_0\langle k_\perp^2\rangle/\langle k_\perp^2\rangle_0$. Nontrivial solutions for the orbit correlations follow if Eq. (7) admits positive P solutions. The subscript 0 is adopted for indicating quantities that will pertain in the absence of a shear flow. Following the time scale renormalization (introduced earlier and explained below in detail), we have made the replacements,

$$\overline{\sigma} \to \overline{W}P^\gamma/2, \quad |\widetilde{\sigma}| \to \widetilde{W}P^\gamma/2, \quad \omega \to \omega P^\gamma, \tag{8}$$

where $\overline{W} \equiv |d\overline{v}_E/dr|t_{c0}/\alpha\left\langle \hat{k}_\perp^2\right\rangle^{1-\gamma}$, $\widetilde{W} \equiv |d\widetilde{v}_E/dr|t_{c0}/\alpha\left\langle \hat{k}_\perp^2\right\rangle^{1-\gamma}$, $|d\overline{v}_E/dr|$ is the static shear flow, and $|d\widetilde{v}_E/dr|$ is the amplitude of the oscillatory shear flow.

The notation used in Eq. (8) reflects our time scale renormalization. Recall that the standard normalization of the time scale in terms of turbulence de-correlation time (for example, simply taking t_c to be $\approx 1/D\langle k_\perp^2\rangle$) will be inappropriate for representing a "measure" of shear flow suppression. To properly account for the effective de-correlation time pertaining to a system with shear flow, we have chosen the representative diffusion coefficient

$$D = D^*\langle\psi^2\rangle^\gamma, \tag{9}$$

where D^* stands for the part of diffusion independent of turbulence level $\langle\psi^2\rangle$. The appropriate time scale for effects of shear flow on turbulence should be defined by the de-correlation time with zero shear flow, $t_{c0} \equiv 1/2D_0\langle k_\perp^2\rangle_0$, where $D_0 = D^*\langle\psi^2\rangle_0^\gamma$. It is widely accepted that $\gamma = 1$ is characteristic of weak turbulence regime, $\gamma = 0.5$ is characteristic of strong turbulence regime, and the plausible physical regime for γ lies between 0.5–1.

Studies of a few limiting cases of Eq. (7) yield the following quick results:

(1) When we have only pure oscillatory shear flow ($\overline{W} = 0$), turbulence is found to be suppressed ($P^{-1} < 1$ implies suppression),

$$P = \frac{1}{4}\left(1 + 3\sqrt{1+\frac{\Delta_1}{3}}\right) \xrightarrow[\Delta_1 << 1]{} 1 + \frac{\Delta_1}{8}. \tag{10}$$

(2) In large ω ($\gg 1$) limit, the "suppression" due to time-varying shear flow alone is given by

$$P = \frac{1}{4}\left(1 + 3\sqrt{1+\frac{32\widetilde{W}^2}{3\omega^2}}\right), \tag{11}$$

indicating that the higher the oscillatory frequency, the weaker the effect towards suppression. In the limit ω going to infinity, P goes to unity (no suppression). This result is qualitatively consistent with previous studies.[5,6]

(3) In the large static shear limit ($\overline{W} \gg 1$), we find

$$P^{-1} = \left(\sqrt{3/2}(1-\Delta_3)\overline{W}\right)^{-2/(3-2\gamma)}, \tag{12}$$

showing that the time-varying flow (contained in Δ_3) tends to diminish the static shear flow suppression.

The analytical characteristic equation, Eq. (7), can also be solved numerically; the real positive solution being the only ones of physical interest. For zero time-varying

component ($\widetilde{W}=0$, and thereof $\Delta_1,\Delta_2,\Delta_3=0$), the present results reduce to those of Ref. 4.

For co-existing static and time-varying components, the numerical results clearly display, what may be termed, mutual exclusiveness in turbulence suppression caused by the static and time varying components of the shear flow. In the 3D Fig. 1 (vertical coordinate = turbulence suppression level (P^{-1}), and the two horizontal coordinates are for static ($\overline{W}$) and time-varying ($\widetilde{W}$) shear flow, respectively), one can see a ridge appearing along the diagonal line, indicating weaker suppression as the two flows become comparable. This feature as well as other suppression characteristics are qualitatively similar to the numerical results based on a Floquet analysis. No comparison will be given here. It may be remarked, though, that the above analytical theory gives acceptable results if the frequency is not too low (say, ω not lower than 3). The analytical results become quite accurate as ω exceeds 6.

For lower frequency range, one must employ numerical methods to solve the basic equation set depicted in Eq. (1); it can be put into the standard form,

$$\dot{\boldsymbol{q}}(t)=\mathbf{A}(t)\boldsymbol{q}(t), \tag{13}$$

where

$$\mathbf{A}(t)=\begin{pmatrix}1/4 & 3/4 & 0\\ 3/4 & 1/4 & 4\sigma\\ 2\sigma & 0 & -1/2\end{pmatrix}, \tag{14}$$

with $\sigma=\overline{\sigma}+|\widetilde{\sigma}|\cos\omega t$. The three components of vector $\boldsymbol{q}(t)$ stand for the orbit correlation $\langle X_-^2(\tau)\rangle$, $\langle \overline{Y}_-^2(\tau)\rangle$, and $\langle X_-(\tau)\overline{Y}_-(\tau)\rangle$, respectively.

In the Floquet theory of differential equation with periodic coefficients, the general solution is expressible in terms of a periodic function multiplied with an exponential factor, wherein the constant coefficient is usually referred to be the Floquet index. It is the real positive Floquet index (corresponding to the real positive root of characteristic equation with constant coefficient) that describes the interesting time scale in which the turbulent fluid elements fall apart. Numerically, one needs to solve the eigen-values (ρ_1,ρ_2,ρ_3) of the monodromy operator $\boldsymbol{Q}(T)$ (the matrix composed of three independent solutions of vector $\boldsymbol{q}(t)$) with $T\equiv 2\pi/\omega$.[9] The following identity

$$\rho_1\rho_2\rho_3=\exp\left[\int_0^T ds\,\mathrm{Tr}\mathbf{A}(s)\right]\to 1 \tag{15}$$

is used as a validity check of numerical program. It is a consequence of the fact that the matrix $\mathbf{A}(t)$ is traceless.

Each eigen-value (the exponential factor of the general solution) corresponds to one Floquet index. Let us choose ρ_1 corresponding to real positive Floquet index P (the other two roots ρ_2 and ρ_3 correspond to the Floquet indices of complex conjugate with negative real part). Because of time scale renormalization (see Eq. (8)), the coefficient of equation is really the function of the solution (through the Floquet index corresponding to ρ_1). This nonlinear problem is solved using a shooting code.

The phenomena of mutual exclusiveness of turbulence suppression between the static and time-varying shear flow can be well exhibited in the 3D Fig. 1 ($\overline{W}$, $\widetilde{W}$, and $P^{-1}\equiv\langle\psi^2\rangle/\langle\psi^2\rangle_0\langle k_\perp^2\rangle/\langle k_\perp^2\rangle_0$) alluded to earlier. We plot the numerical solutions of Eq. (14) and Eq. (8) (based on Floquet theory) for a given parameter set: $\gamma=1$, $\omega=0.25$. The ridge along the diagonal line from $(\widetilde{W},\overline{W})=(0,0)$ to $(\widetilde{W},\overline{W})=(3,3)$ characterizes the mutual exclusiveness between the two; the exclusiveness is maximized around the diagonal line as the strengths of the two components $(\widetilde{W},\overline{W})$ get closer.

In Fig. 2, the turbulence suppression is displayed for various $\overline{W}=1.5$, 3, 6 versus $\widetilde{W}/\overline{W}$ for $\gamma=1$, $\omega=0.25$ in a manner similar to Fig. 4 of the simulations presented in

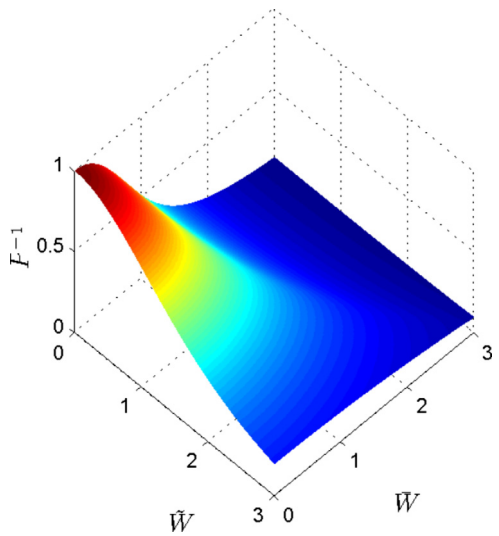

FIG. 1. (Color online) The turbulence suppression $P^{-1}\equiv\langle\psi^2\rangle/\langle\psi^2\rangle_0\langle k_\perp^2\rangle/\langle k_\perp^2\rangle_0$ versus static shear flow $\overline{W}$ and oscillatory shear flow $\widetilde{W}$ for the parameter set $\gamma=1$, $\omega=0.25$. The computation is based on the Floquet theory.

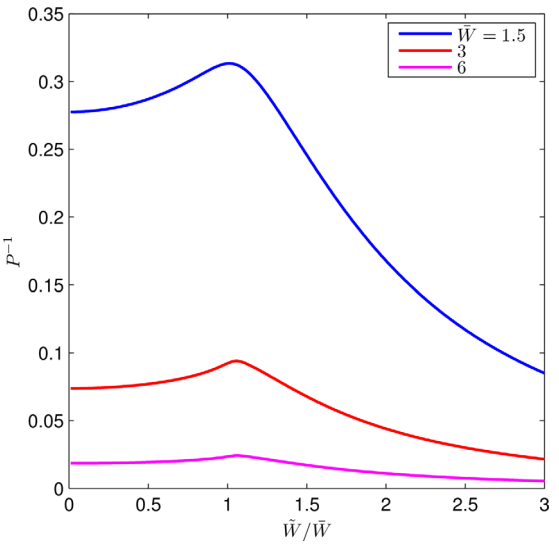

FIG. 2. (Color online) The turbulence suppression $P^{-1}\equiv\langle\psi^2\rangle/\langle\psi^2\rangle_0\langle k_\perp^2\rangle/\langle k_\perp^2\rangle_0$ versus the ratio of oscillatory to static shear flow $\widetilde{W}/\overline{W}$ for $\gamma=1$, $\omega=0.25$ and various $\overline{W}=1.5$, 3, and 6. The computation is based on the Floquet theory.

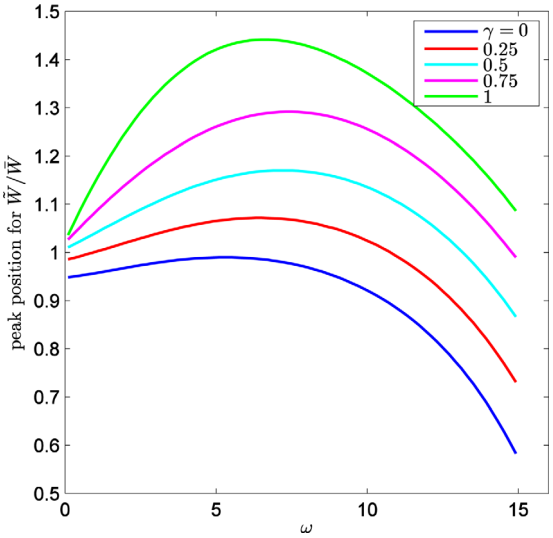

FIG. 3. (Color online) The dependence of peak position $\widetilde{W}/\overline{W}$ in Fig. 2 on oscillatory frequency ω for various $\gamma = 0$, 0.25, 0.5, 0.75, 1.0, and $\overline{W} = 3$. The computation is based on the Floquet theory.

Ref. 6. The location of peaks is very close to and in good agreement with the results of Ref. 6, provided the maximal transport is identified with minimal turbulence suppression. On the other hand, for lower $\overline{W}$, for example $\overline{W} < 1$, no peak appears. There might exist corresponding counterparts in the simulation; however, results in this range are not displayed in Ref. 6.

It is also interesting to see, as illustrated in Fig. 3, the low frequency condensation of the peak position in $\widetilde{W}/\overline{W}$ to 1 when the frequency of oscillatory shear flow approaches zero for various parameters. In other words, the minimal turbulence suppression does not, always, occur when the two components are equal; minimum suppression value is parameter dependent unless the frequency of oscillatory shear flow is sufficiently low.

We conclude this brief article with a few remarks on experimental observations regarding L-H transition on tokamaks. In recent years, it is reported that the GAMs may be playing a deactivating role in the L-H transition occurring in ASDEX-U, DIII-D, and EAST.[10–12] The GAM excited in L phase seems to get totally quenched in the H-phase. For example, on EAST, GAM observed in L mode at a frequency 12–15 kHz disappeared completely after transition to H mode. At the same time, the power in low frequency part of the spectrum was enhanced in H mode, while the power content in the frequency range 20 kHz–200 kHz was suppressed down by one order of magnitude.[12] It is thus an interesting question to ask if GAM and H mode are mutually exclusive? Initially, such a question may sound peculiar, since GAM, as a type of shear flow, was supposed to suppress turbulence. Why do the GAMs, then, seem to reverse their role? It is their elimination, rather than presence, which might stimulate transition to the H-mode. The following simple picture seems to emerge from our analysis—If GAMs were present by themselves alone, then indeed they would suppress turbulence and hasten L-H transition—But in most cases of interest, they appear along with the "time independent" shear flows. In such cases, the GAMs work against the "well recognized" turbulence suppressing ability of the "static" one and, in fact, must be marginalized to allow the "static" shear flow to work their magic to cause an L-H transition. Naturally, in a "static" shear flow created H-phase, there is no room for any sizable GAMs to persist.

The authors would like to thank Professor C. X. Yu and Dr. A. D. Liu for drawing their attention to the cited experiments. This work was supported by ITER-China Program No. 2010GB107000 (YZZ), National Magnetic Confinement Fusion Science Program (China) under Grant No: 2009GB101002 (TS), and USDOE Contract No. DE-FG 03-96ER-54366 (SMM).

[1]P. H. Diamond, S.-I. Itoh, K. Itoh, and T. S. Hahm, Plasma Phys. Controlled Fusion **47**, R35 (2005).
[2]H. Biglari, P. H. Diamond, and P. W. Terry, Phys. Fluids B **2**, 1 (1990).
[3]K. C. Shaing, E. C. Crume, Jr., and W. A. Houlberg, Phys. Fluids B **2**, 1492 (1990).
[4]Y. Z. Zhang and S. M. Mahajan, Phys. Fluids B **4**, 1385 (1992); *ibid.* **B5**, 2000 (1993).
[5]T. S. Hahm, M. A. Beer, Z. Lin, G. W. Hammett, W. W. Lee, and W. M. Tang, Phys. Plasmas **6**, 922 (1999).
[6]S. Maeyama, A. Ishizawa, T.-H. Watanabe, M. M. Škorić, N. Nakajima, S. Tsuji-Iio, and H. Tsutsui, Phys. Plasmas **17**, 062305 (2010).
[7]T. Xie, Y. Z. Zhang, and A. K. Wang, Nucl. Fusion Plasma Phys. **31**, 105 (2011) (in Chinese with English abstract).
[8]N. N. Bogoliubov and Y. A. Mitropolsky, *Asymptotic Methods in the Theory of Non-linear Oscillations*, 2nd ed. (Hindustan Publishing Corporation, Delhi, 1961), Chap. V.
[9]C. Chicone, *Ordinary Differential Equations with Applications* (Springer, New York, 2006), Chap. II, p. 191.
[10]G. D. Conway, C. Angioni, F. Ryter, P. Sauter, J. Vicente, and ASDEX Upgrade Team, Phys. Rev. Lett. **106**, 065001 (2011).
[11]G. R. McKee1 *et al.*, Nucl. Fusion **49**, 115016 (2009).
[12]C. X. Yu and A. D. Liu, private communication (May 2011).